



## Irradiation effects on the $C-V$ and $G/\omega-V$ characteristics of Sn/p-Si (MS) structures

Ş. Karataş<sup>a,\*</sup>, A. Türit<sup>b</sup>, Ş. Altındal<sup>c</sup>

<sup>a</sup> Department of Physics, Faculty of Sciences and Arts, University of Kahramanmaraş Sütçü İmam, 46100 Kahramanmaraş, Turkey

<sup>b</sup> Department of Physics, Faculty of Sciences and Arts, Atatürk University, 25240 Erzurum, Turkey

<sup>c</sup> Department of Physics, Faculty of Arts and Sciences, Gazi University, 06500 Ankara, Turkey

### ARTICLE INFO

#### Article history:

Received 30 October 2007

Accepted 14 September 2008

#### Keywords:

<sup>60</sup>Co gamma-rays

$C-V$  and  $G/\omega-V$  characteristics

Series resistance

Interface states density

Si

### ABSTRACT

In this paper, we have investigated the effects of <sup>60</sup>Co gamma ( $\gamma$ )-ray source on the electrical properties of Sn/p-Si metal–semiconductor (MS) structures using the capacitance–voltage ( $C-V$ ) and conductance–voltage ( $G/\omega-V$ ) measurements before and after irradiation at room temperature. The MS structures were investigated in the frequency range 20–700 kHz irradiation effects on the electrical properties of Sn/p-Si MS structures before irradiation, and after irradiation, these structures were exposed to <sup>60</sup>Co  $\gamma$ -ray source irradiation with the dose rate of 2.12 kGy/h and the total dose range was 0–500 kGy at room temperature. It was found that the  $C-V$  and  $G/\omega-V$  curves were strongly influenced with both frequency and the presence of the dominant radiation-induced defects, and the series resistance was increased with increase in dose. On the other hand, the interface state density ( $N_{ss}$ ) as depended on radiation dose and frequency was determined from  $C-V$  and  $G/\omega-V$  measurements, and the interface states densities decreased with increase in frequency and radiation dose.

© 2008 Elsevier Ltd. All rights reserved.

### 1. Introduction

Silicon (Si) was the first material used for solar cells in space and it has remained the most popular choice ever since due to its history of reliable performance. The investigations in this work are of utmost importance for their applications in space and radiation environments. Thus, the metal–semiconductor (MS) structures, metal–insulator–semiconductor (MIS)-type structures or solar cells and metal–oxide–semiconductor (MOS) capacitors are extremely sensitive to high-energy radiation (such as <sup>60</sup>Co gamma ( $\gamma$ )-ray and high-energy electrons, neutrons and ions). The MS structure-based devices are sensitive to the electrical properties of the MS interface and any mechanism that affects the interface also influences the performance of these devices (Aboelfotoh, 1989; Karataş and Türit, 2006; Kumar and Kanjilal, 2006; Singh et al., 2000).

Radiation effects on MS structures have attracted large attention during the last decades, and a variety of studies have been performed by many authors (Aboelfotoh, 1989; Karataş and Türit, 2006; Kumar and Kanjilal, 2006; Singh et al., 2000; Feteha, 2000; Feteha et al., 2002; Tataroğlu and Altındal, 2006; Ferraglio and Anderson, 1979; Willoughby, 1994; Karataş et al., 2005). These investigations are of most importance for their applications in

space and radiation environment. The studies on the effect of  $\gamma$  irradiation in semiconductor devices are of technological importance and scientific interest. The most common source of  $\gamma$  rays for irradiation processing comes from the radioactive isotope <sup>60</sup>Co  $\gamma$ -ray source irradiation. It is manufactured specifically for the  $\gamma$  irradiation process.

The  $\gamma$  rays pass through the materials being irradiated depositing energy causing electrons to be shifted to a higher energy state or removed completely from the atom. This effect, ionization, can produce a number of different characteristics depending on the chemical structure of the material. It is known that <sup>60</sup>Co  $\gamma$ -ray irradiation at the interface causes modification of the interface and affects the electrical characteristics of the MS structure formed on the semiconductor. Thus, when irradiative particles (gamma, electrons, protons, etc.) enter the MS, they cause a considerable amount of lattice damage (vacancies, defects, etc.). These defects are mainly acting as recombination centers resulting in a reduction in the carrier's diffusion length (Feteha, 2000; Feteha et al., 2002; Tataroğlu and Altındal, 2006). The diffusion length of the MIS-Si solar cell could be degraded by up to 96% in a manner similar to p–n Si solar cells under the same proton irradiation dose (Ferraglio and Anderson, 1979; Willoughby, 1994).

The capacitance–voltage ( $C-V$ ) and conductance–voltage ( $G/\omega-V$ ) characteristics of a metal–semiconductor structure are extremely sensitive to interface state density at the MS interface. Deep understanding of the physical properties of the materials

\* Corresponding author. Tel.: +90 344 219 1310; fax: +90 344 219 1042.

E-mail address: [skaratas@ksu.edu.tr](mailto:skaratas@ksu.edu.tr) (Ş. Karataş).

under the influence of radiation exposure is vital for the effective design of MS devices (Arshak and Korostynska, 2004; Tuğluoğlu, 2007). The electrical characteristics of MS structures in the Schottky barrier diodes have been studied more than that in the MIS-type Schottky diodes due to the existence of a native insulator layer between metal and semiconductor that passivates the surface of the semiconductor. The improvements in radiation resistance of MS, MIS and solar cells are necessary for widespread applications.

In this work, as different from previous works (Karataş and Türüt, 2006; Karataş et al., 2005), we have investigated effects of the  $^{60}\text{Co}$   $\gamma$ -ray source on the electrical properties of Sn/p-Si (MS) structures using the C–V and  $G/\omega$ –V measurements before and after irradiation at room temperature. In addition, before and after irradiation, we investigated the effects of the series resistance and interface states, which cause non-ideal behaviour on the electrical properties of the MS structure.

## 2. Experimental

The MS structures were prepared using p-type silicon wafers with (100) surface orientation, 2" in diameter and 6.248  $\Omega\text{cm}$  resistivity. The wafer was chemically cleaned using the RCA cleaning procedure. The RCA cleaning procedure was as follows: a 10 min boil in  $\text{NH}_3+\text{H}_2\text{O}_2+6\text{H}_2\text{O}$  followed by a 10 min boil in  $\text{HCl}+\text{H}_2\text{O}_2+6\text{H}_2\text{O}$ . The RCA cleaning with HF dip shows a predominant coverage of the surface with hydride groups. The native oxide on the front surface of the substrate was removed in  $\text{HF}:\text{H}_2\text{O}$  (1:10) solution for 30 s and finally the wafer was rinsed in deionized water for 30 s. Then, low-resistivity ohmic back contact to p-type Si (100) wafers was made by using Al, followed by a temperature treatment at 570  $^\circ\text{C}$  for 3 min in  $\text{N}_2$  atmosphere. The Schottky contacts were formed by evaporation of Sn dots with a diameter of about 1.5 mm (diode area =  $1.76 \times 10^{-2} \text{ cm}^2$ ). All evaporation processes were carried out in a turbo molecular fitted vacuum coating unit at about  $10^{-7}$  Torr.

The C–V and  $G/\omega$ –V measurements were performed by using the HP 4192A LF impedance analyzer (5 Hz–13 MHz) and the test signal of 40 mV<sub>rms</sub>. All measurements (C–V and  $G/\omega$ –V) were performed in the dark before and after  $^{60}\text{Co}$   $\gamma$ -ray source irradiation with the dose rate of 2.12 kGy/h and the total dose range was 0–500 kGy at room temperature. The measurements were carried out with the help of a microcomputer through an IEEE-488 ac/dc converter card.

## 3. Results and discussion

### 3.1. Frequency dependency of capacitance-voltage (C–V) and conductance-voltage ( $G/\omega$ –V) measurements

The C–V and  $G/\omega$ –V characteristics of Sn/p-type Si structure at the frequency range of 20–700 kHz at room temperature are shown in Figs. 1 and 2, respectively. As shown in Figs. 1 and 2, the measured C–V and  $G/\omega$ –V plots are dependent on both the bias voltage and frequency. In the depletion and accumulation regions for a given applied voltage, the C and  $G/\omega$  increase with decrease in frequencies due to the time-dependent response of interface states. In addition, each C–V curve has three different regions of accumulation–depletion–inversion region. The C–V curves give peak in the depletion region due to the particular distribution of interface states between Sn/p-type Si interface and effect of series resistance. The position of peaks in the C–V curves is shifting towards the reverse bias region with increasing frequency and almost disappears at high frequencies. This occurs because at

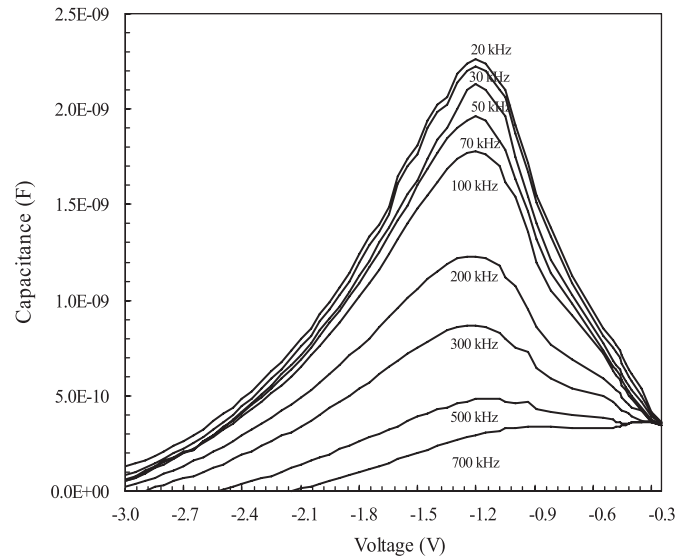


Fig. 1. The C–V characteristics of the Sn/p-Si structure at various frequencies.

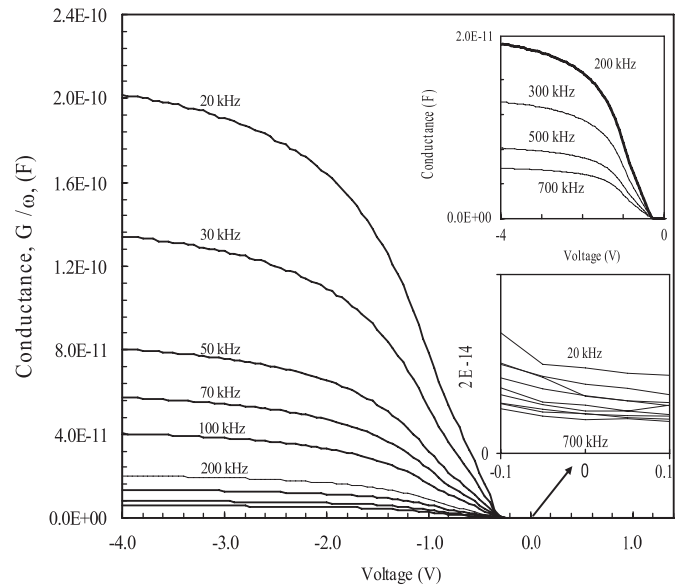


Fig. 2. The  $G/\omega$ –V characteristics of the Sn/p-Si structure at various frequencies.

lower frequencies the interface states can follow the ac signal and yield an excess capacitance, which depends on the frequency. In the high-frequency limit ( $f \geq 700 \text{ kHz}$ ), however, the interface states cannot follow the alternating current (ac) signal. This makes the contribution of interface state capacitance to the total capacitance negligibly small (Hill and Coleman, 1980; Akkal et al., 2000; Gökçen et al., 2008; Karataş and Türüt, 2004).

Fig. 2 shows the measured  $G_m/\omega$ –V characteristics of Sn/p-type Si structure at different frequencies. Conductance technique is based on the conductance losses resulting from the exchange of majority carriers between the interface states and majority carrier band of the semiconductor when a small ac signal is applied to the semiconductor devices (Nicollian and Goetzberger, 1965). In Fig. 2, when the frequency increases from 20 to 700 kHz, the conductance decreases from  $9.55 \times 10^{-15} \text{ F}$  ( $= 0.00955 \text{ pF}$ ) to  $7.73 \times 10^{-15} \text{ F}$  ( $= 0.00773 \text{ pF}$ ) at zero bias, and thus, the  $G/\omega$ –V plots for high frequencies and forward bias voltages became almost constant. From the above argument it can be concluded that

under bias voltage the interface states ( $N_{ss}$ ) are responsible for the observed frequency dispersion in  $C-V$  and  $G/\omega-V$  plots.

In this study, frequency dependence of interface states densities were obtained using the Hill–Coleman method (Hill and Coleman, 1980). In general, the interface states in equilibrium with the semiconductor do not contribute to the capacitance at sufficiently high frequencies, because the charge at the interface states cannot follow the ac signal and, in this case, the MS structure is the only space charge capacitance. According to Hill and Coleman (1980), the density of interface states can be calculated by using the following equation:

$$N_{ss} = \frac{2}{qA} \frac{(G_m/\omega)_{\max}}{((G_m/\omega)_{\max} C_{ox})^2 + ((1 - C_m)/C_{ox})^2} \quad (1)$$

where  $A$  is the diode area,  $\omega$  is the angular frequency,  $C_m$  and  $(G/\omega)_{\max}$  are the measured capacitance and conductance which correspond to the peak values, respectively, and  $C_{ox}$  is the capacitance of the insulator layer and can be obtained from  $C-V$  and  $G/\omega-V$  measurements in the strong accumulation region. As seen in Fig. 3, interface states density exponentially decreases with increase in frequency. At low frequencies, as can clearly be seen from Fig. 3, the interface states density strongly depends on frequency. Thus, the high values of interface states at low frequencies were attributed to an increase in the capacitance of the diode. However, at high frequencies, interface states density became almost constant. Therefore, the values of the capacitance at the high-frequency region originate from only space charge capacitance, and at higher frequencies (as described above)

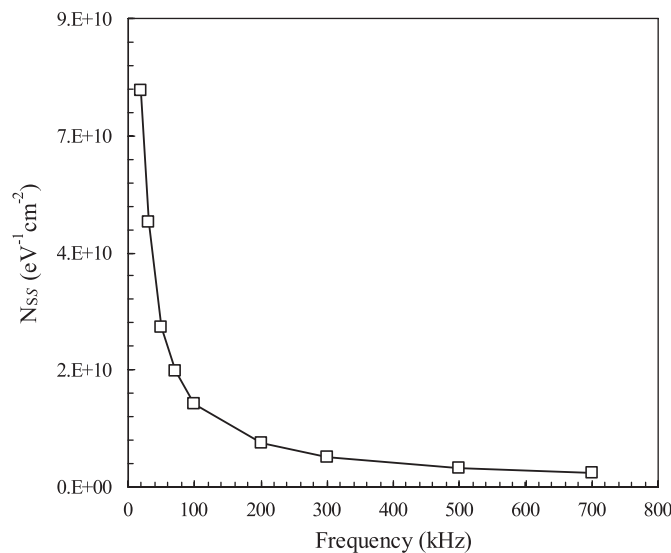


Fig. 3. Frequency dependence of the interface states densities deduced from  $C-V$  and  $G/\omega-V$  measurements.

interface states cannot follow the ac signal. Furthermore, the values of various parameters for Sn/p-Si MS structure determined from  $C-V$  and  $G/\omega-V$  characteristics in the frequency range of 20–700 kHz are given in Table 1. As can be seen in Table 1, as the frequency increases further, the values of  $C$  and  $G/\omega$  are found to decrease, so do the values of  $N_{ss}$ .

The real series resistance of MS devices can be subtracted from the measured capacitance and conductance measurements in the strong accumulation region at high frequency (Nicollian and Goetzberger, 1967). The frequency dependency of the series resistance can be obtained from the measurements of  $C-V-f$  and  $G/\omega-V-f$  curves (Nicollian and Goetzberger, 1967):

$$R_s = \frac{G_{ma}}{G_{ma}^2 + (\omega C_{ma})^2} \quad (2)$$

where  $G_{ma}$  and  $C_{ma}$  are values of the conductance and capacitance obtained in the strong accumulation region at high frequency ( $f \geq 500$  kHz). Using Eq. (2), the values of  $R_s$  were calculated as a function of voltage at various frequencies as shown in Fig. 4. As can be clearly seen from Fig. 4, the series resistance depends on both frequency and voltage and gives a peak at a voltage which decreases with the increase in frequency. The voltage and frequency dependence of  $R_s$  is attributed to the particular distribution density of interface states and interfacial insulator layer (Rhoderick and Williams, 1988).

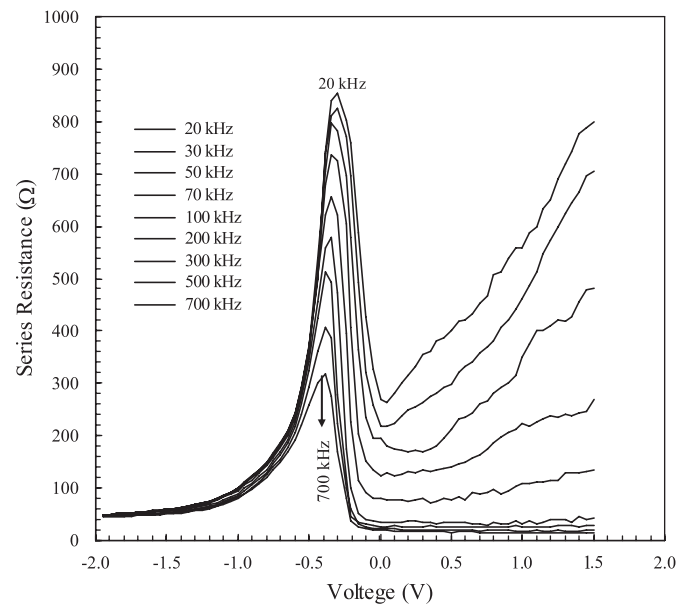


Fig. 4. The series resistance–voltage ( $R_s-V$ ) plot of the Sn/p-Si structure at various frequencies.

Table 1

The experimental values of the Sn/p-Si Schottky structure obtained at various frequencies

$f$ (kHz)	$V_{\max}$ (V)	$C_m$ ( $\times 10^{-9}$ F)	$(G_m/\omega)$ ( $\times 10^{-11}$ F)	$R_s$ ( $\Omega$ )	$N_{ss}$ ( $\times 10^{10}$ eV $^{-1}$ cm $^{-2}$ )
20	−1.2	2.26	10.5	75.9	7.457
30	−1.2	2.25	7.01	75.6	4.979
50	−1.2	2.13	4.24	74.9	3.011
70	−1.2	1.96	3.06	74.1	2.173
100	−1.2	1.78	2.18	72.7	1.548
200	−1.2	1.23	1.15	68.6	0.816
300	−1.2	0.87	0.79	65.9	0.563
500	−1.2	0.41	0.50	62.9	0.365
700	−1.2	0.29	0.36	61.4	0.261

### 3.2. Radiation dependency of capacitance-voltage (C–V) and conductance-voltage ( $G/\omega$ –V) measurement

The irradiation sources' damage occurs through two basic mechanisms: bulk damage, which is due to the displacement of atoms from their lattice sites, and surface damage, which is due to the charge build-up in the surface layers of the MS structures (Luukka, 2006). Figs. 5 and 6 show the measured C–V and  $G/\omega$ –V characteristics of the Sn/p-Si structure at room temperature and 500 kHz for devices irradiated from 10 to 500 kGy, respectively. It is seen that the general nature of variation of C–V and  $G/\omega$ –V plots obtained as frequency dependence in Figs. 1 and 2, and the variation of C–V and  $G/\omega$ –V plots (Figs. 5 and 6) obtained after

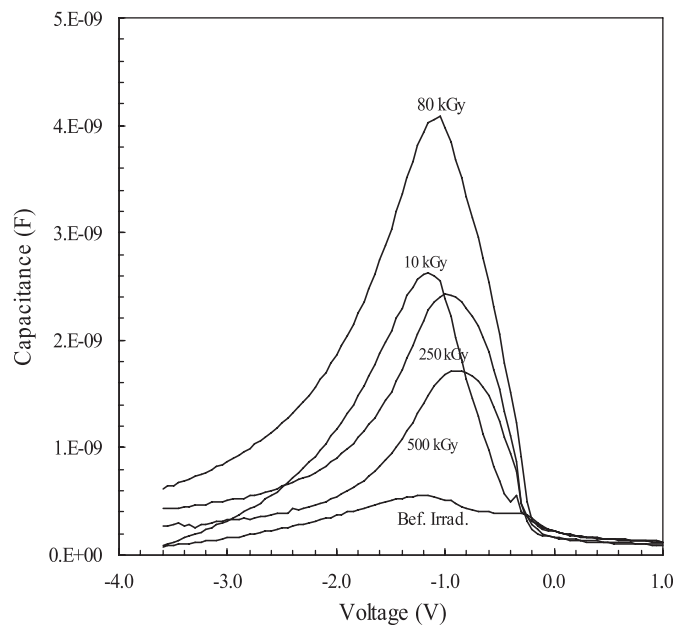


**Fig. 5.** The C–V characteristics of the Sn/p-Si structure at various frequencies after  $\gamma$ -ray irradiation.

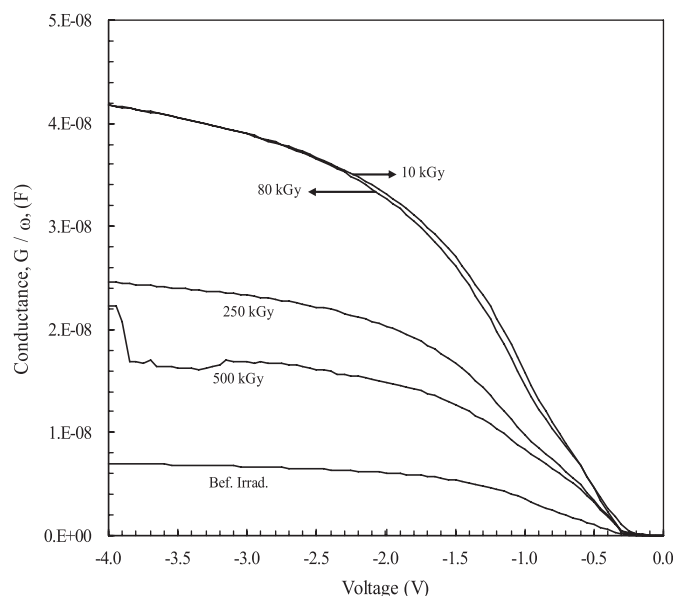
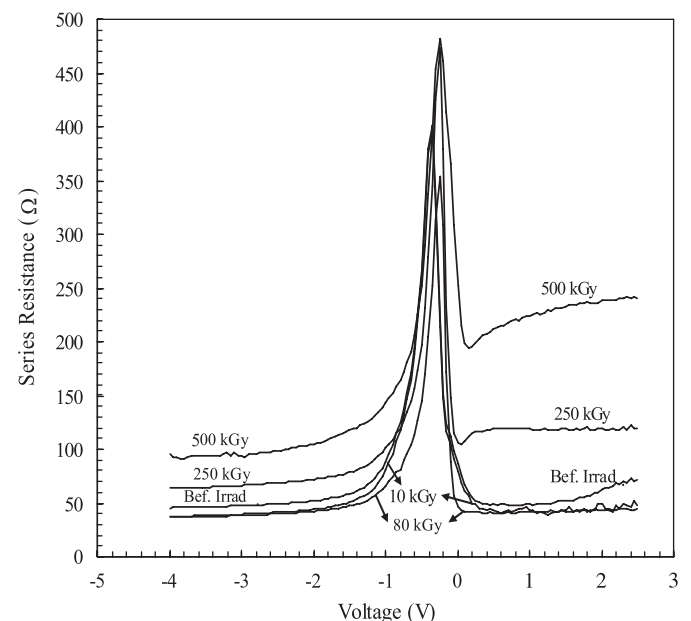


**Fig. 6.** The  $G/\omega$ –V characteristics of the Sn/p-Si structure at various dose ranges after  $\gamma$ -ray irradiation.

radiated condition are similar. The after-irradiation C–V variation shifts a little towards the right. On the other hand, the after-irradiation  $G/\omega$ –V variation decreases a little with radiation. This state is due to the radiation-induced change in the flat band voltage of the devices, as reported in Chauhan and Chakrabarti (2002). The event radiation-induced net change in the interface state and oxide charges favour the bending of the band and causes inversion to occur at a lower applied voltage. The irradiation-induced excess carriers generated in the substrate depend on the dose rate and are responsible for change in capacitance of the MS device under exposure to irradiation (Chauhan and Chakrabarti, 2002).

The series resistance is an important parameter to designate the noise ratio of the device as dependent on the irradiation dose. Therefore, both the real values and voltage dependence of the series resistance  $R_s$  were calculated from Eq. (2) according to Nicollian and Goetzberger (1967) and at various doses ranging from 10 to 500 kGy are shown in Fig. 7. As described above, the series resistance gives a peak in approximately the same voltage range. The values of series resistance of the Sn/p-Si structure at the strong accumulation region for the device irradiated from before irradiation kGy to 500 kGy were obtained as 76.98, 68.88, 59.24, 109.65, and 152.29  $\Omega$ . As shown in Fig. 7 and Table 2, the series resistance increases with increase in radiation dose. This behaviour of the series resistance has been attributed to particular distribution of interface state (Karataş and Türüt, 2006; Karataş et al., 2005; Rhoderick and Williams, 1988). At the same time, these values of series resistance indicate that special attention should be given to the effects of series resistance in the application of the C–V and  $G/\omega$ –V measurements.

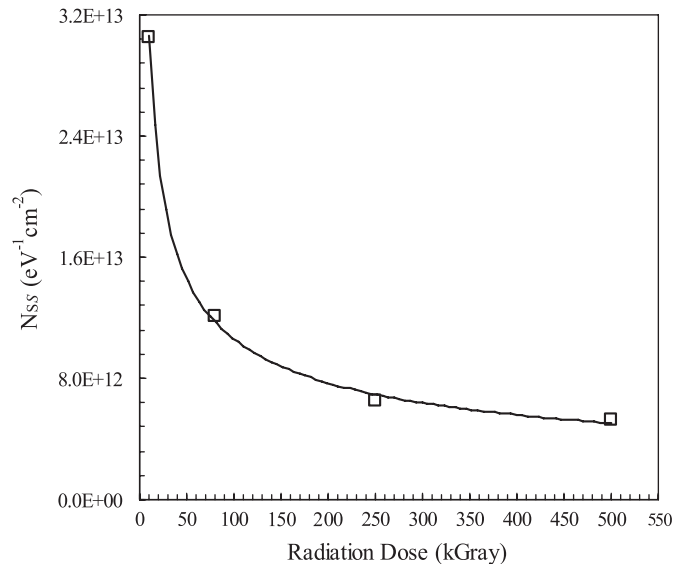
The density of interface states can be obtained from Eq. (1) using the measured capacitance and conductance values after radiation. Fig. 8 shows the changes of interface states densities at various irradiation doses of the Sn/p-Si structure after  $\gamma$ -ray irradiation from a  $^{60}\text{Co}$  source. The values of interface states densities ( $N_{ss}$ ) in the radiation dose range of 0–500 kGy are given in Table 2. As shown in Table 2,  $N_{ss}$  slightly decreases with increase in radiation dose. The interface states' densities decrease with increase in radiation dose, being attributed to the decrease in the recombination centers and the passivation of the Si surface



**Fig. 7.** The series resistance–voltage ( $R_s$ –V) of the Sn/p-Si structure at various dose ranges after  $\gamma$ -ray irradiation.

**Table 2**The experimental values of the Sn/p-Si Schottky structure obtained at various dose ranges after  $\gamma$ -ray irradiation

Irradiation (kGy)	$V_{\max}$ (V)	$C_m (\times 10^{-9} \text{ F})$	$(G_m/\omega) (\times 10^{-8} \text{ F})$	$R_s (\Omega)$	$N_{ss} (\times 10^{13} \text{ eV}^{-1} \text{ cm}^{-2})$
Bef. irradi.	−1.1	0.54	0.40	76.98	0.0050
10	−1.1	2.60	1.85	68.88	3.05
80	−1.1	4.06	1.71	59.24	1.21
250	−0.9	2.42	0.91	109.65	0.65
500	−0.9	1.71	0.73	152.29	0.52

**Fig. 8.** Irradiation dependence of interface states densities obtained from the C–V and  $G/\omega$ –V measurements at different  $\gamma$ -ray doses.

due to the existence of the native insulator layer between the metal and the semiconductor.

#### 4. Conclusion

The frequency dependence C–V and  $G/\omega$ –V characteristics of the Sn/p-Si structures were investigated in the frequency range of 20–700 kHz. The experimental results confirmed that both the measured C and  $G/\omega$  vary with applied voltage and frequency, and decrease with increase in frequency in the depletion and accumulation region due to a continuous distribution of the interface states between the metal and the semiconductor. The higher values of capacitance and conductance at low frequency were attributed to the excess capacitance resulting from the interface states, which is in equilibrium with the p-Si that can follow the ac signal. The series resistance curves give a peak, decreasing with increasing frequencies. Furthermore, it has been shown that the interface states' density strongly depends on frequency, and exponentially decreases with increasing frequencies. In addition, the effects of  $\gamma$ -ray irradiation on the C–V and  $G/\omega$ –V characteristics of the Sn/p-Si structures were investigated. Experimental results show that the exposure to increasing cumulative  $\gamma$ -ray doses has the following effects: (a) an increase in the change of C and  $G/\omega$  due to the irradiation-induced defects at the interface, (b) an increase in the series resistance obtained

from C–V and  $G/\omega$ –V measurements, and (c) an increase in the interface state densities  $N_{ss}$  after low irradiation doses followed by a monotonic reduction of  $N_{ss}$  with increasing dose. The results indicate that the degradation in the Sn/p-Si structure properties may be due to the introduction of radiation-induced interfacial defects (between Sn and p-Si), and lattice defects via displacement damage.

#### References

- Aboelfotoh, M.O., 1989. Influence of thin interfacial silicon oxide layers on the Schottky-barrier behaviour of Ti on Si(100). *Phys. Rev. B* 39, 5070–5078.
- Akkal, B., Benamara, Z., Gruzza, B., Bideux, L., 2000. Characterization of interface states at Au/InSb/InP(100) Schottky barrier diodes as a function of frequency. *Vacuum* 57, 219–238.
- Arshak, K., Korostynska, O., 2004. Thin film pn-junctions based on oxide materials as  $\gamma$ -radiation sensors. *Sens. Actuat. A: Phys.* 113, 307–311.
- Chauhan, R.K., Chakrabarti, P., 2002. Effect of ionizing radiation on MOS capacitors. *Microelectron. J.* 33, 197–203.
- Ferraglio, R., Anderson, W.A., 1979. Proton radiation effects on Cr–MIS single crystal Si-solar cell. *Appl. Phys. Lett.* 35, 18–20.
- Feteha, M.Y., 2000. Gamma radiation effect on the GaAs solar cell performance. *IEEE Int. Symp. Compd. Semicond.*, 91–96.
- Feteha, M.Y., Soliman, M., Gomaa, N.G., Ashry, M., 2002. Metal–insulator–semiconductor solar cell under gamma irradiation. *Renewable Energy* 26, 113–120.
- Gökçen, M., Tataroğlu, A., Altındal, Ş., Bülbül, M.M., 2008. The effect of  $^{60}\text{Co}$  ( $\gamma$ -ray) irradiation on the electrical characteristics of Au/SnO<sub>2</sub>/n-Si (MIS) structures. *Radiat. Phys. Chem.* 77, 74–78.
- Hill, W.A., Coleman, C.C., 1980. A single frequency approximation for interface state density determination. *Solid-State Electron.* 23 (9), 987–993.
- Karataş, Ş., Türüt, A., 2004. The determination of interface state energy distribution of the H-terminated Zn/p-type Si Schottky diodes with high series resistance by the admittance spectroscopy. *Vacuum* 74, 45–53.
- Karataş, Ş., Türüt, A., 2006. Electrical properties of Sn/p-Si (MS) Schottky barrier diodes to be exposed to  $^{60}\text{Co}$   $\gamma$ -ray source. *Nucl. Instrum. Methods Phys. Res. A* 566, 584–589.
- Karataş, Ş., Türüt, A., Altındal, Ş., 2005. Effects of  $^{60}\text{Co}$   $\gamma$ -ray irradiation on the electrical characteristics of Au/n-GaAs (MS) structures. *Nucl. Instrum. Methods Phys. Res. A* 555, 260–265.
- Kumar, S., Kanjilal, D., 2006. Barrier height modification of Au/n-Si Schottky structures by swift heavy ion irradiation. *Nucl. Instrum. Methods Phys. Res. B* 248, 109–112.
- Luukka, P.R., 2006. Helsinki Institute of Physics, Internal Report Series, Annual Report, HIP, 2006–04.
- Nicollian, E.H., Goetzberger, A., 1965. MOS conductance technique for measuring surface states parameters. *Appl. Phys. Lett.* 7 (8), 216–219.
- Nicollian, E.H., Goetzberger, A., 1967. The Si–SiO<sub>2</sub> interface-electrical properties as determined by the MIS conductance technique. *Bell Syst. Tech. J.* 46, 1055–1133.
- Rhoderick, E.H., Williams, R.H., 1988. *Metal–Semiconductor Contacts*, second ed. Clarendon, Oxford.
- Singh, R., Arora, S.K., Singh, J.P., Singh, F., Kanjilal, D., 2000. Swift heavy ion irradiation induced modification of current–voltage characteristics of heavily doped Au/n-GaAs Schottky diode. *IEEE Semiconducting Insulating Mater. Conf. SIMC-XI*, 167–170.
- Tataroğlu, A., Altındal, Ş., 2006. Electrical characteristics of  $^{60}\text{Co}$   $\gamma$ -ray irradiated MIS Schottky diodes. *Nucl. Instrum. Methods Phys. Res. B* 252, 257–262.
- Tuğluoğlu, N., 2007.  $^{60}\text{Co}$   $\gamma$ -ray irradiation effects on the interface traps density of tin oxide films of different thicknesses on n-type Si (111) substrates. *Nucl. Instrum. Methods Phys. Res. B* 254, 118–124.
- Willoughby, A.F.W., 1994. The control of radiation in space solar cells. *Int. J. Electron.* 76, 865–882.